# Exploring the Dynamical Behavior of Spin Waves Through Energy-Absorption Interferometry

Felix Biggs

May 7, 2015

**Abstract**

Energy absorption interferometry can be used to find the natural dynamical modes of a system of interacting magnetic dipoles, using only measurements of total absorbed power. This is of enormous utility in the investigation of magnetic properties of nanoscale and thin-film systems, areas of great technological significance and contemporary research interest, due to their use in magnetic storage media and spintronic devices. Previously used to investigate interacting electric dipoles, it is a general technique based on the physics of partially coherent energy absorption [8], and has been theoretically shown applicable to systems of interacting magnetic dipoles. Here simulations based on the discrete dipole approximation (DDA) are shown, illustrating this in practice, comparing it to other techniques such as Ferromagnetic Resonance (FMR), and to demonstrate some of the properties of such systems. Experimental realization requires only a static applied field, scannable phase locked sources, and an ability to measure absorbed power; these are simple requirements which make the method highly practicable at a range of frequencies. The modes may be found for a range of applied fields and mapped spatially, using our knowledge of the forms of the source impressed fields, revealling yet more about the system.

## 1 Introduction

Magnetic properties of thin films are an active area of research both for their use in elucidating our understanding of magnetism and because of their enormous technological importance [2].

As an example of how quickly developments in this area influence the technology sector, the giant magnetoresistive effect (GMR) was discovered in 1988 (leading to the award of the 2007 Nobel Prize in Physics) and was demonstrated in a hard disk drive read head by 1994, being commercialized shortly thereafter. Between the introduction of the first hard disk drive in 1956 to 2007, there was a $10^8$ increase in magnetic recording density. This progress depends on decreasing the magnetic grain sizes, but demanding problems must be solved as

nanoscale sized structures are reached - inevitably leading to a desire for greater understanding of the fundamental physics involved[3].

## 1.1 Spin Waves

Fundamentally, magnetism arises from the Pauli exclusion principle coupling electron orbitals to spin states. This exchange interaction can be phenomenologically written by treating atoms as directly coupled dipoles, or as a mean field in the rigid band model of metals [3]. Spin waves are coherent excitations of these magnetic dipoles, with scale lengths from $O(10^{-4})$m to $O(10^{-8})$m and characteristic frequencies from gigahertz to terahertz [1]. Their spectrum is highly dependent on the intrinsic system properties and can yield useful information about g-factors, saturation magnetization and exchange couplings [3]. They were originally studied in bulk materials but recently focus has shifted towards engineering microscopic band gaps to perform operations such as data manipulation and storage as described above. There is also much current research in spintronics, a field combining electrical and magnetic manipulation of spins system in solid-state devices, and driven by range of potential applications, such as a circularly polarised spin laser [7].

At low frequencies they are mediated by dipole-dipole interactions and at high frequencies exchange interactions. They can be created by applying a large static field and a small time varying field to a magnetic material - the static field causes the dipoles to align, or at least form domains, and the time-varying field causes excitations. They may also be excited thermally by phonons (central to understanding the destruction of magnetic order, of key importance in magnetic storage media), or by visible or radio frequency photons, allowing for experimental investigation [3]. For a more visual picture we may use a semi-classical model in which the dipoles precess on the surfaces of cones about the direction of the applied field. The low-lying elementary excitations have successive spins advanced in phase by a constant angle, giving the form of a disturbance that propagates as a wave [5, 6].

A recent advance is the development of processes to create magnetic nanoparticles with control of sizes and shapes, with great potential technological application. The determination of their normal modes and ability to control them has important technological implications; an example is that read head size is fundamentally limited by spin-wave noise, which could be reduced by suitable design choices [4].

## 1.2 Current Experimental Techniques

Typically we are interested in scale sizes and forms of dynamical modes and their responsitivites.

Measurement of very small samples can be challenging due to the amount of material. A number of techniques are commonly used to investigate general magnetic properties, including: SQUID magnetometers, x-ray magnetic circular dichroism (XMCD), using the magnetoopic Kerr effect (MOKE) and other

specialist techniques. More direct investigation of the spin wave dynamics may be achieved through the Brillon light scattering and ferromagnetic resonance (FMR) techniques [3].

Ferromagnetic resonance, one of the most useful contemporary techniques, is at microwave frequencies similar in principle to nuclear spin resonance (NMR). In a strong applied magnetic field spins precess and the transmission of radio frequency (RF) or x-ray energy is attenuated, dependent on the relation between precession and applied frequencies. The field strength is varied and attenuation is measured [10]. In a ferromagnetic sample, the transverse susceptibility is large and the strong exchange coupling tends to suppress dipolar contributions so resonance lines may be quite sharp [6]. It gives useful information about dispersion and damping but is difficult to apply to microscopic structures and provides little information about the modes responsible for absorption, for example their spatial forms or degeneracies [1].

## 1.3 Energy Absorption Interferometry

Energy Absorption Interferometry (EAI) was first proposed in the context of electric dipoles and is a general technique for studying modes based on the physics of coherent energy absorption [8]. It is a generalisation of holography in magnetic systems.

The general setup is similar to FMR, with the structure under test placed in a large static magnetic field. It differs in that rather than one source, instead a pair of phase-locked time-varying sources - say magnetic dipoles - are used to probe the system, and the total power absorbed by the is measured. This is dependent on the phase difference between the sources, giving a fringe in power absorption. The complex visibility of this fringe is measured for pairs of source locations.

From this, the technique is able to reconstruct the dynamical modes and their relative responsivities. This can be done for any given source frequency and applied field, and may further be repeated for a range of applied field strengths. Degenerate excitations may be seperated, giving information about system symmetries, and the spatial forms of the modes may be mapped using knowledge of the impressed field forms. We may thus yield a huge amount of useful information about the system.

## 1.4 Experimental Realization

The simplicity of the technique, requiring only phase-locked sources and a measurement of the total absorbed power absorbtion, makes it realizable in a variety of experimetal setups. It is even applicable to different situations entirely, such as the already demonstrated electric dipoles. Here we will describe one possible implementation.

A thin sample is supported by a thermally isolated Si membrane, and bolometer technology is used to very sensitively measure the absorbed power. This is placed in a large static magnetic field from a DC solenoid and illuminated by a

Figure 1: Schematic of a possible experimental apparatus for performing EAI. Arrows represent the collection of precessing, interacting dipoles on top of the substrate. Sources are shown as current-driven loops and an applied field is provided by the coil.

pair of phase-locked magnetic sources which are rotated around the periphery, exciting spin waves. In practice these sources might simply be slightly offset in frequency and the oscillation of power absorption measured to find the phase (already demonstrated in the electronic case[9]).

For the purposes of its reconstruction, the system is treated as a discrete set of magnetic dipoles, which may be fundamental excitations or elements of the discrete dipole approximation (DDA), a versatile technique often used to model scattering. [1, 8]

# 2 Theory

The theory of EAI and its application to magnetic dipoles was initially laid out by Stafford Withington [1, 8].

## 2.1 Spin Waves

The system is modelled as a discrete system of magnetic dipoles. This may be done for any system using the discrete dipole approximation (DDA) - the equation then represents averages over finite macroscopic regions. A single dipole with magnetic dipole moment $\mathbf{m_j}$ will evolve according the Landau-Lifshitz-Gilbert equation:

$$\frac{d\mathbf{m_j}}{dt} = -\gamma_j \mu_0 \mathbf{m_j} \times \mathbf{H}_j^{tot} + \frac{\alpha_j}{|\mathbf{m_j}|}(\mathbf{m_j} \times \frac{d\mathbf{m_j}}{dt}) \tag{1}$$

$j$ is an index which specifies a dipole, $\mathbf{H}_j^{tot}$ is the total magnetic field at the dipole, $\gamma_j$ is the gyromagnetic ratio of the dipole (positive and negative values corresponding to opposite rotation directions) and $\alpha_j$ is a phenomenological damping coefficient (in FMR, for the transverse components of the dynamic part of the magnetization). This equation could be generalized to a Bloch equation with different longitudinal and transverse dampings but this will not be done to simplify the analysis.

Move to the steady state by writing $\mathbf{H}_j^{tot} = \mathbf{H}_j^{tot\,(0)} + \mathbf{H}_j^{tot\,(t)}$, representing the non-time dependent and time dependent terms provided by the large static field and the smaller RF sources respectively. Thus when only the static field is present, the system equilibrates into a state $\mathbf{m_j}^{(0)}$ with no torque on dipoles (from LLG). Generally, the dipoles can form non-aligned domains but we assume they are in the saturated state: all totally aligned with the static field, so $\mathbf{m_j}^{(0)} = m^s \hat{\mathbf{k}}$ (the saturated magnetization), and $\mathbf{H}^{tot(0)} \equiv H^0 \hat{\mathbf{k}} \approx \mathbf{H}^{ext(0)}$. We

also make the vital assumption that in the steady state, all of the absorbed (or indeed extracted) power is transferred from substrate (physically, its phonon system).

We use periodic RF sources so that $\mathbf{H}_j^{tot\,(t)} = \mathrm{Re}\left\{\mathbf{H}_j^{tot\,(1)} e^{-i\omega t}\right\}$. Substituting into LLG and discarding non-linear terms (effectively the approximation $\mathbf{m_j}\cdot\hat{\mathbf{k}} \approx \mathbf{m_j}^{(0)}$, the static component is much greater than the parallel dynamical component) we get:

$$i\frac{\omega}{\gamma\mu_0}\mathbf{m}^{(1)} = m^s\hat{\mathbf{k}} \times \mathbf{H}^{tot\,(1)} + \mathbf{m}^{(1)} \times H^0\hat{\mathbf{k}} + i\frac{\omega\alpha}{\gamma\mu_0}\hat{\mathbf{k}} \times \mathbf{m}^{(1)}$$

**Non-Interacting Case**

Inverting the above equation we can write the susceptibility of a system of non-interacting, precessing dipoles with position vectors $\mathbf{r}_{0j}$ as:

$$\overline{\overline{\boldsymbol{\chi}}}_L(\mathbf{r}) = \sum_j \frac{\gamma_j\mu_0 m_j^s\omega}{(\omega_{0j}^2 - \omega^2) - i\omega\Gamma_j}\overline{\overline{\boldsymbol{S}}}_j\delta(\boldsymbol{r} - \boldsymbol{r_{0j}}) \tag{2}$$

with

$$\overline{\overline{\mathbf{S}}}_j = \frac{\omega_{0j}}{\omega}\hat{\boldsymbol{i}}\hat{\boldsymbol{i}} + i\hat{\boldsymbol{j}}\hat{\boldsymbol{i}} - i\hat{\boldsymbol{i}}\hat{\boldsymbol{j}} + \frac{\omega_{0j}}{\omega}\hat{\boldsymbol{j}}\hat{\boldsymbol{j}}, \quad S_j = \begin{pmatrix} \omega_0/\omega & -i \\ i & \omega_0/\omega \end{pmatrix}$$

where we have used dyadics and $S_j$ is the matrix form of $\overline{\overline{\mathbf{S}}}_j$ (see appendix for detail). The $\mathbf{m}_j^{(1)}$ are time independent in the plane perpendicular to $\mathbf{H}^{(0)}$. The natural frequency of precession is $\omega_{0j} = \gamma_j\mu_0 H_j^{(0)}$ and the damping rate is $\Gamma_j = 2\alpha_j\omega_{0j}$, and we have assumed low loss (small $\alpha_j$). Now spatial dipole moment is $\mathbf{M}^{(1)}(\mathbf{r}) = \overline{\overline{\chi}}_L(\mathbf{r}) \cdot \mathbf{H}^{ext(1)}(\mathbf{r})$, with no spatial integral or $\mathbf{r}'$ dependence, as the non-interacting case is totally local.

The natural modes of the isolated dipole are found from the eigenvectors and eigenvalues (diagonalisation) of $\overline{\overline{\mathbf{S}}}$:

$$\mathbf{u}_+ = \frac{1}{\sqrt{2}}(\hat{\mathbf{i}} + i\hat{\mathbf{j}}), \quad \lambda_+ = \frac{\omega_0}{\omega} + 1$$

$$\mathbf{u}_- = \frac{1}{\sqrt{2}}(\hat{\mathbf{i}} - i\hat{\mathbf{j}}), \quad \lambda_- = \frac{\omega_0}{\omega} - 1$$

corresponding respectively to rotation in the the natural precession direction, and in the reverse direction,.

**Interacting Case**

We can write $\mathbf{H}_j^{tot} = \mathbf{H}_j^{ext} + \mathbf{H}_j^{xch} + \mathbf{H}_j^{dip}$ where the terms represent the applied external field on the system, the effective field from exchange interactions between dipoles, and the scattered field from the other dipoles.

The exchange interaction effective field at a dipole can be written as:

$$\mathbf{H}_j^{xch} = J \sum_{k=NN} \mathbf{m}_k \tag{3}$$

where NN indicates the nearest neighbors.

The dipole scattering term is:

$$\mathbf{H}^{dip(1)}(\mathbf{r}) = \int \overline{\overline{\mathbf{G}}}(\mathbf{r}, \mathbf{r}') \cdot \mathbf{M}^{(1)}(\mathbf{r}') d\mathbf{r}'$$

using the non-retarded magnetostatic greens dyadic (reference????):

$$\overline{\overline{\mathbf{G}}}(\mathbf{r}, \mathbf{r}') = \frac{1}{R^3} \left( 3\frac{\mathbf{RR}}{R^2} - \bar{\bar{\mathbf{I}}} \right), \quad \mathbf{R} = \mathbf{r} - \mathbf{r}', \quad R = |\mathbf{R}| \tag{4}$$

We may now combine these terms and the non interacting susceptibility to give:

$$\mathbf{H}^{ext(1)}(\mathbf{r}_i) = \sum_j \overline{\overline{\mathbf{T}}}_{ji} \cdot \mathbf{H}^{tot(1)}(\mathbf{r}_j) \tag{5}$$

$$\overline{\overline{\mathbf{T}}}_{ij} = \bar{\bar{\mathbf{I}}}\delta_{ij} - \frac{\gamma_i \mu_0 m_i^s \omega}{(\omega_{0i}^2 - \omega^2) - i\omega\Gamma_i} \left\{ J\delta_{i,NN} \overline{\overline{\mathbf{S}}}_i + (1 - \delta_{ij}) \overline{\overline{\mathbf{G}}}(\mathbf{r}_j, \mathbf{r}_i) \cdot \overline{\overline{\mathbf{S}}}_i \right\}$$

which can be written as a matrix equation in the dipole locations, and inverted to give the total field at each dipole in terms of the applied field.

**Power Absorption**

Since EAI uses power absorption measurements, calculation of them is needed. In the explicitly time dependent and real case, the instantaneous power absorption is:

$$P(t) = \mu_0 \int \mathbf{H}(\mathbf{r}, t) \cdot \frac{\partial \mathbf{M}(\mathbf{r}, t)}{\partial t} d^3\mathbf{r}$$

Using the definition of non-local susceptibility,

$$\mathbf{M}(\mathbf{r}) = \int \overline{\overline{\boldsymbol{\chi}}}(\mathbf{r}, \mathbf{r}') \cdot \mathbf{H}(\mathbf{r}') d^3\mathbf{r}'$$

the time average power absorption is

$$P(\nu) = \frac{\omega}{2} \mu_0 \mathrm{Im} \int_V \mathbf{H}^*(\mathbf{r}) \cdot \mathbf{M}(\mathbf{r}) d^3\mathbf{r} = \frac{\omega}{2} \mu_0 \mathrm{Im} \int_V \int_V \mathbf{H}^*(\mathbf{r}) \cdot \overline{\overline{\boldsymbol{\chi}}}(\mathbf{r}, \mathbf{r}') \cdot \mathbf{H}(\mathbf{r}') d^3\mathbf{r} d^3\mathbf{r}' \tag{6}$$

over the volume of the sample, $V$, since the susceptibility elsewhere is zero.

For our system of dipoles we thus find a power absorption:

$$P(\nu) = \sum_j \frac{\gamma_j \mu_0^2 m_j^s}{2} \left[ \frac{\omega \Gamma_j}{\omega^2 (\frac{\omega_{0j}^2}{\omega^2} - 1)^2 + \Gamma_j^2} \right] \times \mathbf{H}_j^{tot(1)*} \cdot \overline{\overline{\mathbf{S}}_j} \cdot \mathbf{H}_j^{tot(1)} \tag{7}$$

If the system is rotationally excited, $\mathbf{H}^{tot(1)}(\mathbf{r}_i) = a\mathbf{u}_\pm$, the absorbed power will be

$$< P(a\mathbf{u}_\pm) >= \frac{1}{2}a^2\Gamma\gamma\mu_0^2 m_s \frac{\omega(\omega_0/\omega \pm 1)}{\omega^2(\omega_0^2/\omega^2 - 1)^2 + \Gamma^2}$$

We see from the numerator that the power is always positive for rotation with the natural precession direction, and reaches a peak at $\omega = \omega_0$. However, for the opposite direction rotations, the power is zero at $\omega = \omega_0$, and work may be done by the system for $\omega > \omega_0$, taking energy out of the dipole. Physically the steady state case makes perfect sense for the natural precession rotation direction rotation - however here our assumption of steady state is called into question - the negative power modes would be quickly damped by the applied field removing the energy in an experiment.

In practice, there is nothing wrong with this - modes fall into two separable subsets with opposite rotation directions - there are no mixed modes. The negative power absorption modes would however be much more difficult to detect experimentally due to this rapid damping effect, but we are not generally interested in them either. We focus on the positive absorption, natural precession direction modes.

## 2.2 EAI

After a number of steps from the above forms for the power we may arrive at the most useful form:

$$< P(\nu) >= \frac{\omega}{2}\mu_0 \int_V \int_V \overline{\overline{\mathbf{C}}}^{tot}(\mathbf{r}, \mathbf{r}') \cdot \cdot \overline{\overline{\boldsymbol{\chi}}}^{R}(\mathbf{r}, \mathbf{r}') d^3\mathbf{r} d^3\mathbf{r}' \tag{8}$$

where we have defined $\overline{\overline{\boldsymbol{\chi}}}^{R}(\boldsymbol{r}, \mathbf{r}') = -i\overline{\overline{\boldsymbol{\chi}}}^{A}(\boldsymbol{r}, \mathbf{r}')$ with $\overline{\overline{\boldsymbol{\chi}}}^{A}$ the antihermitian part of $\overline{\overline{\boldsymbol{\chi}}}$ (this makes the power real and discards the non-absorbing hermitan part of $\overline{\overline{\boldsymbol{\chi}}}$); and the magnetic field correlation dyadic, an expectation value across an ensemble of systems (not required for coherent sources), is:

$$\overline{\overline{\mathbf{C}}}(\mathbf{r}, \mathbf{r}') =< \mathbf{H}(\mathbf{r})\mathbf{H}^*(\mathbf{r}') > \tag{9}$$

The double dot is a full contraction to a scalar.

This clearly has the form of an inner product in the abstract vector space of dyadic fields. The power absorbed is the projection of the magnetic field correlation dyadic onto the susceptibility dyadic.

### Non-Scattered Case

If a source at $\mathbf{r}_n$ produces the field $\mathbf{h}_n(\mathbf{r})$, and we have $N$ possible source positions, we produce a basis $\mathbb{A} = \{\mathbf{h}_n(\mathbf{r}), \forall n \in 1...N\}$. We can then write the matrix elements of $\overline{\overline{\boldsymbol{\chi}}}^{R}(\boldsymbol{r}, \mathbf{r}')$ in the basis, and approximately (or exactly, if the source fields span the basis of absorption) reconstruct it using the dual vector set:

$$\chi_{nm} = \int_V \int_V \mathbf{h}_n^*(\mathbf{r}) \cdot \overline{\overline{\boldsymbol{\chi}}}^R(\mathbf{r}, \mathbf{r}') \cdot \mathbf{h}_m(\mathbf{r}') d^3\mathbf{r} d^3\mathbf{r}'$$

$$\overline{\overline{\boldsymbol{\chi}}}^R(\mathbf{r}, \mathbf{r}') \approx \sum_{nm} \chi_{nm} \tilde{\mathbf{h}}_m(\mathbf{r}) \tilde{\mathbf{h}}_m^*(\mathbf{r}') \tag{10}$$

Since we can find the dual set $\tilde{\mathbb{A}}$ numerically from knowing the forms of the impressed fields, if we know the matrix elements $\chi_{nm}$, we can find the response dyadic and diagonalize it to find the natural modes of the system.

It turns out we can do this using only power measurements: this is the beauty of EAI. We illuminate the sample with two fully coherent sources so that:

$$\mathbf{H}^{ext}(\mathbf{r}_j) = \mathbf{h}_n + \mathbf{h}_m e^{-i\Delta\phi}$$

where $\Delta\phi$ is a phase that we may rotate. We then find that the absorbed power becomes:

$$< P(\nu) >= \frac{k_0 Z_0}{2} \left\{ \chi_{nn} + \chi_{mm} + 2|\chi_{nm}| \cos\left[\Delta\phi + \arg(\chi_{nm})\right] \right\}$$

Thus $\chi_{nm}$ is a hermitan matrix, and we may measure the on diagonal terms directly from the power absorbance from each source, and the off diagonal terms by sweeping the phase between the sources and measuring the resulting fringe in the power.

**Scattering**

In the scattered case the total field is a linear function of the impressed field and can be written as:

$$\mathbf{H}(\mathbf{r}) = \int_V \overline{\overline{\mathbf{G}}}(\mathbf{r}, \mathbf{r}') \cdot \mathbf{H}^{ext}(\mathbf{r}') d^3\mathbf{r}'$$

were $\overline{\overline{\mathbf{G}}}(\mathbf{r}, \mathbf{r}')$ is the scattering operator which may be calculated from the magnetostatic Green's function. Since the integral is only over the sample volume, we may regard $\overline{\overline{\mathbf{G}}}(\mathbf{r}, \mathbf{r}')$ as intrinsic to the sample and following a similar analysis to above, we find that:

$$< P(\nu) >= \frac{\omega}{2} \mu_0 \int_V \int_V \overline{\overline{\mathbf{C}}}^{ext}(\mathbf{r}, \mathbf{r}') \cdot \cdot \, \overline{\overline{\mathbf{K}}}(\mathbf{r}, \mathbf{r}') d^3\mathbf{r} d^3\mathbf{r}'$$

where

$$\overline{\overline{\mathbf{K}}}(\mathbf{r}, \mathbf{r}') = \int_V \int_V \overline{\overline{\mathbf{G}}}^{\dagger}(\mathbf{r}, \mathbf{s}) \cdot \overline{\overline{\boldsymbol{\chi}}}^R(\mathbf{s}, \mathbf{s}') \cdot \overline{\overline{\mathbf{G}}}(\mathbf{s}', \mathbf{r}') d^3\mathbf{s} d^3\mathbf{s}'$$

Thus the scattering limits the amount of spatial information we may obtain about $\overline{\overline{\boldsymbol{\chi}}}^R(\mathbf{s}, \mathbf{s}')$.

## 2.3 Matrix Formulation

Now that our model is fully discretized, we describe it in terms of matrices. The column vectors $\mathrm{h}^{\mathrm{ext}}, \mathrm{h}^{\mathrm{tot}} \in \mathbb{C}^{2J}$ contain the complex amplitudes of the transverse cartesian field components of the external and total fields at the position of the dipoles.

Clearly from (5) we can write $\mathrm{h}^{\mathrm{tot}} = \mathrm{T}^{-1}\mathrm{h}^{\mathrm{ext}}$, and also from (8):

$$P = \frac{\omega}{2}\mu_0(\mathrm{h}^{\mathrm{tot}})^\dagger \chi^R \mathrm{h}^{\mathrm{tot}}$$

$$< P >= \mathrm{Tr}\left[\mathrm{C}^{\mathrm{tot}}\mathrm{N}\right], \qquad \mathrm{N} = \frac{\omega}{2}\mu_0\chi^R$$

where we have taken then trace of a number and used the cyclic property to write $\mathrm{C}^{\mathrm{tot}} =< \mathrm{h}^{\mathrm{tot}}(\mathrm{h}^{\mathrm{tot}})^\dagger >$.

Thus, we write the power in terms of the external field:

$$P = \frac{\omega}{2}\mu_0(\mathrm{h}^{\mathrm{tot}})^\dagger \chi^R \mathrm{h}^{\mathrm{tot}} = \frac{\omega}{2}\mu_0(\mathrm{h}^{\mathrm{ext}})^\dagger(\mathrm{T}^{-1})^\dagger \chi^R(\mathrm{T}^{-1})\mathrm{h}^{\mathrm{ext}} = (\mathrm{h}^{\mathrm{ext}})^\dagger \mathrm{L}\mathrm{h}^{\mathrm{ext}}$$

$$< P >= \mathrm{Tr}\left[\mathrm{C}^{\mathrm{ext}}\mathrm{L}\right] \tag{11}$$

Since $\mathrm{C}^{\mathrm{ext}}$ and L are hermitian, they may be diagonalized: $\mathrm{C}^{\mathrm{ext}} = \sum_i \alpha_i \mathrm{f}_i \mathrm{f}_i^\dagger$, $\mathrm{L} = \sum_i \beta_i \mathrm{g}_i \mathrm{g}_i^\dagger$. The power is then

$$< P >= \sum_{ij} \alpha_i \beta_j \left|\mathrm{f}_i^\dagger \mathrm{g}_j\right|^2$$

which describes how the impressed field modes project onto the system modes.

### Closer examination of L

We may look more closely at exactly where L comes from and how it may be incrementally built up. We have a column vector $\mathrm{m} \in \mathbb{C}^{2J}$ containing the transverse components of the dipole moments. If exchange interactions are present then:

$$\mathrm{m} = \chi_L \mathrm{h}^{\mathrm{ext}} + \chi_L \mathrm{G}^{\mathrm{xch}}\mathrm{m} = (\chi_L^{-1} - \mathrm{G}^{\mathrm{xch}})^{-1} \equiv \xi \mathrm{h}^{\mathrm{ext}} \tag{12}$$

where $\mathrm{G}^{\mathrm{xch}}$ is the exchange interaction from (3) and $\chi$ is simply the local susceptibility.

Next we include dipole-dipole scattering, with (4) giving us $\mathrm{G}^{\mathrm{dip}}$:

$$\mathrm{h}^{\mathrm{tot}} = \mathrm{h}^{\mathrm{ext}} + \mathrm{G}^{\mathrm{dip}}\mathrm{m} = (1 - \mathrm{G}^{\mathrm{dip}}\xi)^{-1} \equiv \kappa \mathrm{h}^{\mathrm{ext}} \tag{13}$$

defining $\kappa$, and giving $m = \xi\kappa h^e$.

Thus

$$\mathrm{L} = \frac{\omega}{2}\mu_0 \kappa^\dagger \xi^R \kappa \tag{14}$$

where $\xi^R$ is the hermitian part of $-i\xi$.

## 2.4 Reconstruction with EAI

If the matrix $\mathrm{H}^{\mathrm{ext}} \in \mathbb{C}^{2J\times 2N}$ is made up of columns containing the fields $\mathrm{h}^{\mathrm{ext}}$ associated with particular possible sources. If these impressed fields span the absorption modes, the response matrix can be written in terms of the duals:

$$\mathrm{L} = \sum_{nm} a_{nm} \tilde{\mathrm{h}}_{\mathrm{n}}^{\mathrm{ext}} \tilde{\mathrm{h}}_{\mathrm{m}}^{\mathrm{ext}\dagger} = \tilde{\mathrm{H}}\mathrm{A}\tilde{\mathrm{H}}^{\dagger} \tag{15}$$

so A gives the response in the basis of the sources.

The power absorbed due to two sources is given by:

$$P = [\mathrm{h}_1^{\mathrm{ext}\dagger} e^{-i\phi_1} + \mathrm{h}_2^{\mathrm{ext}} e^{-i\phi_2}]\,\mathrm{L}\,[\mathrm{h}_1^{\mathrm{ext}} e^{i\phi_1} + \mathrm{h}_2^{\mathrm{ext}\dagger} e^{i\phi_2}]$$

and subbing in the response:

$$P_{nm} = a_{nn} + a_{mm} + a_{nm} e^{i\Delta\phi} + a_{mn} e^{-i\Delta\phi} \tag{16}$$

so we may measure a fringe in the power by rotating the phase, and hence find the matrix elements of A.

### Deconvolution

The matrix A contains the intrinsic absorbances of the dipoles, N, convolved with the scattering and exchange interactions, $\mathrm{T}^{-1}$, and finally the greens function taking the field at the sources to the dipoles. Generally only the final step may be deconvolved, as if we know the source properties we may calculate the forms of the impressed fields and invert them (we are allowed to do this because if we do not have fundamental dipole locations then we use DDA which gives them to us).

The dual vectors are defined by $\mathrm{H}^{\mathrm{ext}\dagger}\tilde{\mathrm{H}}^{\mathrm{ext}} = 1$, but inversion is not possible if J is not equal to N. We use the SVD pseudo-inverse, defined by:

$$\mathrm{H} = \mathrm{U}\Sigma\mathrm{V}^{\dagger} \implies \tilde{\mathrm{H}} = \mathrm{U}\Sigma^{-1}\mathrm{V}^{\dagger}; \qquad \mathrm{H}^{\dagger}\tilde{\mathrm{H}} = \mathrm{U}\Sigma\Sigma^{-1}\mathrm{U}^{\dagger}$$

which correctly accounts for numbers of source positions and sample points. If the basis is complete, or over-complete, the final relation will equal the identity. If it is under-complete, the modes are projected onto a measurement space, a filter is applied (which may be impossible to get rid of due to noise) and then the modes are reconstructed.

The whole process may be done using incremental SVD, where each new measurement increases information until all degrees of freedom are found.

### Coherence

The complex visibility is defined by:

$$\gamma_{nm} = \frac{2a_{nm}}{a_{nn} + a_{mm}}$$

We may plot $|\gamma_{nm}|$ and the argument as a function of position by keeping $n$ fixed whilst varying $m$. The modulus reveals the coherence lengths, areas and volumes through which the sample may absorb energy, and the argument is used to reconstruct the modes using EAI.

# 3 Modeling Methodology

## 3.1 Responses

Henceforth, all calculations were done in the basis with the fields or moments at the dipole locations with $\mathbf{H}^{ext(0)} = 1$ unless otherwise stated, and our units are set such that $\mu_0 = 1$.

A given dipole system is described by an array of dipoles, each specified in terms of $\mathbf{r}_j, \alpha_j, \gamma_j, m_j^s$ (generalized functions to create linear and circular such systems were made).

For a given system the response matrix was calculated as follows:

1. Calculate the local susceptibility (2).
2. Calculate the exchange coupled $\xi$ (12).
3. Calculate the dipole scattering matrix $\mathrm{G}^{\mathrm{dip}}$ using (4) and the response matrix L (13), (14).

Note that the matrices depend on the frequency of excitation, and the applied static field.

Now the absorbed power for a given set of sources was found:

1. Calculate the external field at each dipole from the sources using the Greens Function as a matrix (4).
2. Calculate the magnetic correlation matrix $\mathrm{C}^{\mathrm{ext}}$ (9).
3. Calculate the absorbed power (11).

The absorbed powers from some simple systems were then checked against (7).

## 3.2 Reconstruction with EAI

Next, to reconstruct the responses, we:

1. Assemble a set of sources that will be used for the testing. They may be laid out in a line or a circle or some other shape. For this set assemble the matrix $\mathrm{H}^{\mathrm{ext}}$ using the magnetostatic Green's function (4).
2. For each pair of sources measure the complex visibility as the relative phase is varied. This may be done directly with measurements at $\Delta\phi = 0, \pi/2$ or by sweeping the phase and fitting.
3. Using the above and 16, assemble the matrix A.

4. Use SVD to calculate the dual matrix $\widetilde{\mathrm{H}}^{\mathrm{ext}}$.

5. Calculate the reconstructed response matrix $\mathrm{L}' = \tilde{\mathrm{H}}^{\mathrm{ext}}\mathrm{A}\tilde{\mathrm{H}}^{\mathrm{ext}\dagger}$.

The reconstructed matrix can be compared with the one used to calculate the response in order to quantify how well the modes have been reconstructed.

### 3.3 Further investigation of systems

A number of other possibilities for probing system properties were investigated:

- The frequency response to a single source at a number of possible positions and orientations.
- FMR: the response as the magnetic field is swept for a number of possible single fixed frequency sources.
- Absorbance as a function of position for a single source (swept along a line or in a circle).

System properties were elucidated via:

- Diagonalisation of response matrix and examination of the eigenvectors corresponding to normal modes.
- Frequency-power response to direct excitation of those normal modes.
- Creation of 'movies' with plotted arrows rotating at the phases for a particular excitation and for normal modes.
- Plots of magnetic field strength across the plane for various modes.

## 4 Results and Discussion

### 4.1 Two Dipole System

**Frequency Response**

Firstly we consider the system with two dipoles on the x axis, spaced 0.8 apart with and each with a natural frequency of precession $\omega_0 = 1$, magnetization $\mu_0 m_s = 1$, and damping $\Gamma = 1/16$ at an applied field strength of $\mu_0 H^{(0)} = 1$. They were driven in the steady state by a single, circularly polarized source at $x = y = 2$ so as to excite in-phase and anti-phase modes. We show the resonant coupling as a function of frequency for three different exchange couplings, $J = 0.001, 0.1, 0.4$.

We see that in the case of very weak coupling ($J = 0.001$) the dipoles behave as degenerate independent dipoles with a single lorenzian response, peak at 1 and width 1/16. When the exchange couplings are increased we see the system split into two modes, in phase (lower frequency peak) and anti-phase (transverse components of dipoles in opposite directions at any given time, still rotating in

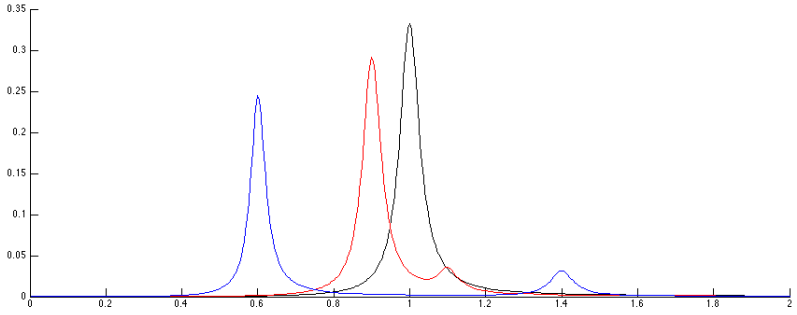


Figure 2: Total power absorption (arb. units) as a function of frequency ($\omega/\omega_0$) for two identical dipoles 0.8 apart with $\Gamma = \omega_0/16$. Lines correspond to exchange couplings $J = 0.001$, 0.1, 0.4 (blue, red, green).

natural precession direction at applied frequency, higher frequency mode). The peaks of the modes are moved by the value of the coupling constant away from the natural frequency $\omega_0$, but they still have the same widths. Note at this source location the in phase mode is more absorbent at its resonant frequency.

Another interesting effect (not shown) is found when the coupling coefficient is very large $J \to 1$. The maximum power absorbances drops to low values as the dipoles effectively screen each other - for the anti-phase mode the dipoles almost cancel each other out, and for the in phase, the peak frequency is very low and hence has low absorbance.

**FMR**

Now we consider the above system with $J = 0.4$, but instead of changing the excitation source frequency we sweep the applied magnetic field (using the fundamental dipole properties $\gamma = 1, \alpha = 1/32$). This done with the same source but at two different frequencies shown, $\omega = 0.8, 1.1$.

Here we see the behavior we expect - the splitting sizes are the same and the peaks occur etc ???

**Fringes and Coherence Lengths/Volumes**

**Reconstruction, Eigenvectors and Spatial Field Strengths**

## 4.2 Linear Systems

Probably easier to do first as fewer degeneracies.

## 4.3 Circular Systems

A few more complicated circular systems (3, 4, 5?)

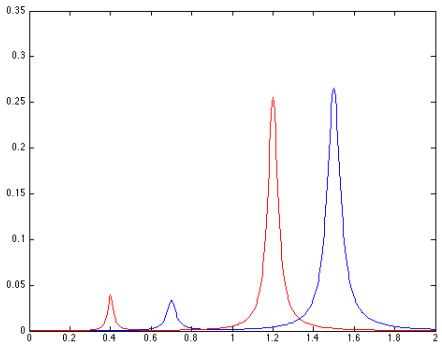


Figure 3: Total power absorption (arb. units) as a function of applied static field for two identical dipoles 0.8 apart, with $\gamma = 1, \alpha = 1/32$. The excitations are provided by sources at $\omega = 0.8, 1.1$ (red, blue).

# 5 Conclusion

A general system was created to simulate the responses of various possible systems of magnetic dipoles, including dipoles arranged in a circle and in a line, and sources to excite them.

Using this it was shown that only a pair of scannable phase locked sources are needed to reconstruct these responses. Using knowledge of the free space forms of the applied magnetic field these responses were mapped back onto the spatial distribution of dipoles, yeilding useful information about the system. This is potentially of great experimental value. To show this, it was demonstrated that it is comparitively difficult to extract such information using more widely used methods, such as ferromagnetic resonance or scanning a single souce across a line.

The properties of such systems were then explored, also serving as a useful test on the validity of the simulations. This was done by plotting frequency responses to, and magnetic field space distributions from, direct excitations of the normal modes. It was found that they behaved as theoretically predicted and a number of points about physical interpretation of the model, for example in the non-steady state opposite precession direction modes. The results were interpreted in light of the geometry of the samples and source configurations and symmetry-induced degeneracies were looked at. This is particularly interesting as such degeneracies cannot be detected via the other methods.

# Appendix

**Notation:**

Vectors (hats for unit vectors): $\mathbf{u}, \mathbf{m}_j, \hat{\mathbf{k}}$

Scalars: $H, \omega$
Dyadics: $\overline{\overline{\chi}}, \overline{\overline{\mathbf{H}}}$
Matrix representations: $\mathrm{h}, \mathrm{H}^{\mathrm{tot}}, \chi$
Dyadics representation???

### A Typical Piece of Code

This is a typical piece of code.

## References


[1] Unpublished Memos - Stafford Withington

[2] Standing Spin Waves in Ultrathin Magnetic Films: A Method to Test for Layer-Dependent Exchange Coupling, J. Rajeswari, H. Ibach, and C.M. Schneider Phys. Rev. Lett. 112, 127202 (http://journals.aps.org/prl/abstract/10.1103/PhysRevLett.112.127202#fulltext)

[3] Magnetism in ultrathin film structures, Vaz Bland & Lauhoff, 2008 Rep. Prog. Phys. 71 056501 (http://iopscience.iop.org/0034-4885/71/5/056501/pdf/0034-4885_71_5_056501.pdf)

[4] Normal Modes of Spin Excitations in Magnetic Nanoparticles, Grimsditch Leaf Kaper Karpeev & Camley, Physical Reveiw B Vol. 69, Iss. 17 1 May 2004 (http://journals.aps.org/prb/pdf/10.1103/PhysRevB.69.174428)

[5] Spin Waves in Ferromagnets, Phillips & Rosenberg, 1966 Rep. Prog. Phys. 29 285 (http://iopscience.iop.org/0034-4885/29/1/307)

[6] Kittel, Introduction to Solid State Physics, 7th Edition

[7] Spintronics: Fundamentals and applications, Zutic Fabian Sarma. (http://arxiv.org/pdf/cond-mat/0405528.pdf

[8] Probing the dynamical behaviour of surface dipoles through energy-absorption interferometry, Withington & Thomas, Physical Review A 86, 043835 (2012)

[9] Experimental Demonstration of an Interferometric Technique for Characterizing the Full Optical Behavior of Multi-Mode Power Detectors, C.N. Thomas, Terahertz Science and Technology, IEEE Transactions on (Volume:2 , Issue: 1 )

[10] Longitudinal Detection of Ferromagnetic Resonance using X-ray Transmission Measurements, Boero et al, (http://infoscience.epfl.ch/record/147825/files/2009_Boero_RSI.pdf)